Organic & Biomolecular Chemistry

Accepted Manuscript

ROYAL SOCIETY OF CHEMISTRY

www.rsc.org/obc

Journal Name

RSCPublishing

ARTICLE

Rare *Streptomyces* sp. polyketides as modulators of K-Ras localisation

Cite this: DOI: 10.1039/x0xx00000x

Angela A. Salim,[‡a] Xue Xiao,[‡a] Kwang-Jin Cho,[b] Andrew M. Piggott,[a†] Ernest Lacey,[c] John F. Hancock[b] and Robert J. Capon*[a]

Received 00th January 2012,
Accepted 00th January 2012

DOI: 10.1039/x0xx00000x

www.rsc.org/

Chemical investigations of a soil-derived *Streptomyces* sp. led to the isolation of five new polyketides, (+)-oxanthromicin, (±)-*hemi*-oxanthromicins A/B, (±)-*spiro*-oxanthromicin A and oxanthroquinone, and the known alkaloid staurosporine, and the detection of four new metastable analogues, (±)-*spiro*-oxanthromicins B1/B2/C1/C2. Among the compounds tested, SAR investigations established the synthetic oxanthroquinone ethyl ester and 3-*O*-methyl-oxanthroquinone ethyl ester were optimal at mislocalising oncogenic mutant K-Ras from the plasma membrane of intact Madin-Darby canine kidney (MDCK) cells (IC_{50} 4.6 and 1.2 μM), while a sub-EC_{50} dose of (±)-*spiro*-oxanthromicin A was optimal at potentiating (750%) the K-Ras inhibitory activity of staurosporine (IC_{50} 60 pM). These studies demonstrate that a rare class of *Streptomyces* polyketide modulates K-Ras plasma membrane localisation, with implications for the future treatment of K-Ras dependent cancers.

Introduction

Ras GTPases are key molecular switches that regulate cell growth, proliferation and differentiation, and are ubiquitously expressed in mammalian cells as three isoforms (H-Ras, N-Ras and K-Ras).[1] Constitutively activated oncogenic K-Ras is a key driver of oncogenesis in pancreatic adenocarcinomas (95%), colon adenomas (40%) and non-small cell lung cancer (15–20%).[2] The key role played by K-Ras in these cancers is evidenced by experimental data, which demonstrate that inhibition of K-Ras membrane localisation blocks all oncogenic activity.[3] Despite K-Ras inhibitors being very attractive prospects as cancer chemotherapeutics, the development of clinically useful inhibitors has proved elusive.

In an effort to address this challenge, we employed a high-throughput, high-content assay to screen a library of microbial extracts, successfully detecting a *Streptomyces* sp. (MST-134270), isolated from a soil sample collected near Pamplona, Spain, as a source of metabolites that selectively mislocalised Ras proteins. In an earlier report,[4] we described staurosporine (**10**) isolated from this culture as a potent and selective inhibitor of K-Ras plasma membrane (PM) localisation, disrupting phosphatidylserine trafficking at concentrations below the threshold required for high affinity pan-kinase activity. This report extends our earlier findings, to describe the spectroscopic analysis, chemistry and biology of compounds **1**–**9** (Fig. 1), including commentary on their biosynthetic origins, chemical stability and total synthesis.

Results and discussion

Bioassay-guided fractionation of a solid phase (cracked wheat) cultivation of MST-134270 resulted in the isolation and characterisation of five new polyketides, (+)-oxanthromicin (**1**), (±)-*hemi*-oxanthromicin A (**2**), (±)-*hemi*-oxanthromicin B (**3**), (±)-*spiro*-oxanthromicin A (**4**), and oxanthroquinone (**9**), as well as the detection and identification of four new metastable analogues, (±)-*spiro*-oxanthromicins B1/B2 (**5**/**6**), and (±)-*spiro*-oxanthromicins C1/C2 (**7**/**8**), and the isolation of the known indole alkaloid staurosporine (**10**) (Fig. 1).

HRESI(–)MS measurements on **1** established a molecular formula of $C_{36}H_{30}O_{12}$ (Δmmu –0.2) while the NMR (DMSO-d_6) data (Fig. 2 and ESI Table S1a) revealed only 18 carbon resonances, necessitating a degree of symmetry. Further analysis of the ^{1}H NMR data revealed resonances for one tertiary methyl (δ_H 1.44), two benzylic methyls (δ_H 2.18 and 2.69), one isolated (δ_H 7.16) and two *ortho* coupled (δ_H 6.33 and 7.12, 7.8 Hz) aromatic protons, and a chelated hydroxy group (δ_H 13.46, s), with diagnostic 2D NMR correlations permitting assembly of a dimeric anthrone featuring a rare peroxide bridge. A search of the literature and comparison of NMR data with the published compound (ESI Table S1b) confirmed that **1** was (+)-oxanthromicin ($[\alpha]_D^{22}$ +157, *c* 0.26, EtOH), a new enantiomer of the rare *Streptomyces* metabolite (–)-oxanthromicin ($[\alpha]_D^{26}$ –172, *c* 0.3, EtOH).[5]

Molecular formulae attributed to **2** ($C_{18}H_{16}O_6$, Δmmu +0.8) and **3** ($C_{19}H_{18}O_6$, Δmmu –0.2) on the basis of HRESI(–)MS measurements were suggestive that both compounds contain

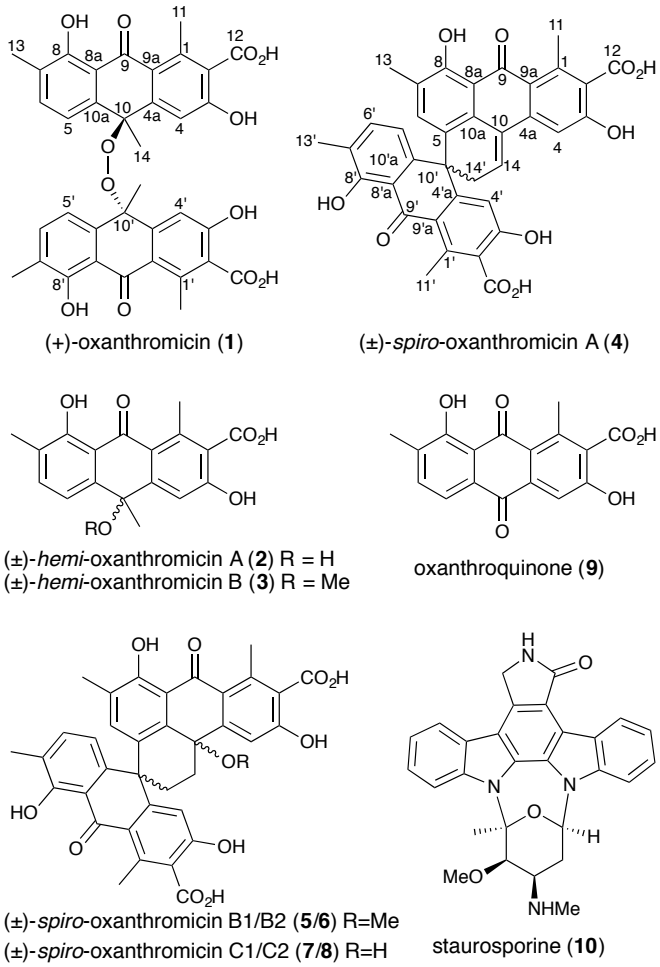

Fig.1 Structures of **1–10**

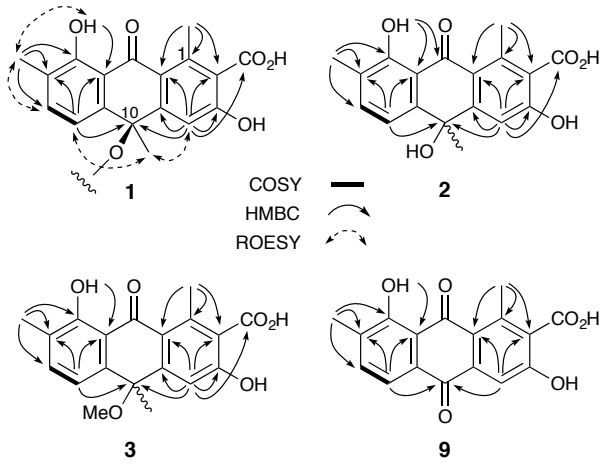

Fig. 2 Selected 2D NMR correlations for **1–3** and **9**

the monomer polyketide unit in **1**. Supportive of this hypothesis, analysis of the NMR (DMSO-d_6) data for **2** and **3** (Fig. 2 and ESI Tables S2–S3) revealed differences centred around replacement of the C-10 peroxy bridge in **1** with (i) a 10-OH (δ_H 6.11) moiety in **2**, exhibiting HMBC correlations to C-4a, C-10 and C-10a and ROESY correlations to H-4 and H-5, and (ii) a 10-OMe (δ_H 2.81, s; δ_C 51.8) moiety in **3**, exhibiting HMBC correlations to C-10 and ROESY correlations to H-4 and H-5. These observations, together with the lack of an optical rotation, permitted assignment of racemic structures to (±)-*hemi*-oxanthromicins A (**2**) and B (**3**) as indicated. Similarly, HRESI(–)MS measurements on **9** ($C_{17}H_{12}O_6$, Δmmu +0.7) together with analysis of the 1D and 2D NMR (DMSO-d_6) data (Fig. 2 and ESI Table S5) permitted assignment of the structure for oxanthroquinone (**9**) as indicated.

HRESI(–)MS measurements established a molecular formula of $C_{36}H_{26}O_{10}$ (Δmmu –0.3) for **4**, while analysis of the NMR (DMSO-d_6) data (Fig. 3 and ESI Table S4), suggested a heavily substituted aromatic system possessing many structural characteristics in common with the co-metabolites **1**–**3**. Detailed analysis of these NMR data, including consideration of diagnostic 2D NMR correlations, permitted assembly of the planar structure as indicated. More specifically, HMBC correlations required that the aromatic methyl H_3-13 be flanked by H-6 and the phenolic 8-OH, while additional correlations linked this fragment to the quaternary aromatics C-8a and C-10a, and the sp^3 *spiro* C-10′. COSY correlations established the H_2-14′ to H-14 fragment, while HMBC correlations linked this fragment to C-10′, C-5, C-10a and C-10. Further HMBC correlations required that the aromatic methyl H_3-11 be flanked by C-2 and C-9a, and *para*-disposed to H-4, which was in turn flanked by C-4a and C-5 (the latter bearing a hydroxy group). Additional HMBC correlations from H-4 to C-10, supported by ROESY correlations between (i) H-6 and H_3-13, (ii) H_3-13 and 8-OH, (iii) 8-OH and H_3-11 and (iv) H-4 and H-14, defined the ABCD ring system as indicated (Fig. 3). Comparable 2D NMR correlations defined the EFG ring system, with diagnostic HMBC correlations linking the *spiro* C-10′ to H-4′, H-5′ and H-6′. ROESY correlations between H-5′ and both H-6 and H_2-14′, and between H-4′ and both H-6 and H_2-14′, defined the orthogonal relationship between the ABCD and EFG ring systems (Fig. 3). Despite the presence of a chiral centre (C-10′), the lack of an optical rotation required that (±)-*spiro*-oxanthromicin A (**4**) be assigned the racemic structure as indicated. Further chemical studies supportive of this structure assignment are presented below.

HPLC-DAD-MS analysis of the crude MeOH extract of *Streptomyces* sp. MST-134270 confirmed the dominant cultivation/biosynthetic products as **1**, **2** and **10**, with **3** and **4** only detected at trace levels (ESI Fig. S10). Significantly, during SPE fractionation, the detected (and recovered) yields of **3** and **4** increased, as did levels of two hitherto undetected compounds **5** and **6**. These observations strongly suggested that **3**–**6** were capable of being produced during handling (ESI Fig. S11). In support of this hypothesis, exposure of a pure sample of **2** to 0.1% TFA/MeOH (conditions comparable to those encountered during SPE fractionation) resulted in partial conversion to **3** and **4**, while exposure to 0.1% TFA/MeCN yielded only **4** (ESI Fig. S12). Likewise, a pure sample of **3** was observed to undergo partial conversion to **2** during routine handling.

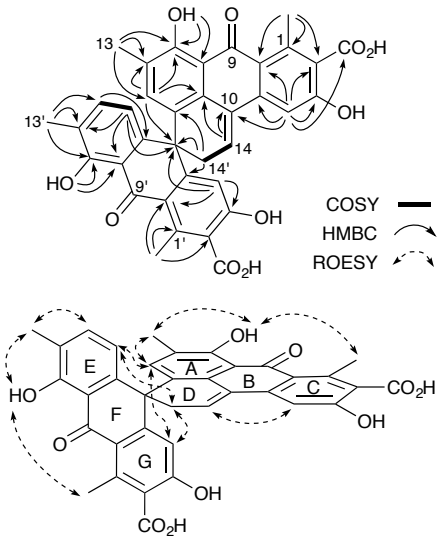

Fig. 3 Selected 2D NMR correlations for **4**

In an effort to assign structures to **5** and **6**, we noted that their UV-vis (DAD) spectra were similar to those of **1**–**3**, suggestive of closely related chromophores and molecular structures, while HPLC-HRESI(–)MS analysis suggested that **5** ($C_{37}H_{30}O_{11}$, Δmmu +2.4) and **6** ($C_{37}H_{30}O_{11}$, Δmmu +2.0) were isomeric MeOH adducts of **4**. Attempts at purification of **5** and **6** by reversed phase HPLC proved problematic as immediately post-elution both underwent partial conversion to **7** and **8**, a transformation that proceeded to near-completion after standing at r.t. for 3 h (ESI Figs. S13–S14). The transformation products **7** and **8** exhibited almost identical UV-vis (DAD) spectra to **5** and **6**, with HPLC-HRESI(–)MS analysis suggesting that **7** ($C_{36}H_{28}O_{11}$, Δmmu +0.6) and **8** ($C_{36}H_{28}O_{11}$, Δmmu +0.0) were isomeric H_2O adducts of **4**. On concentrating *in vacuo* and resuspending in MeOH, the mixture of **7** and **8** rapidly transformed to a complex mixture of **4**–**8**, dominated by **4**.

In presenting a plausible mechanism for the biosynthetic/chemical origins of **1**–**9** (Fig. 4), we speculate that the polyketide precursor, oxanthroquinone (**9**), undergoes stereospecific methylation to a single (10*R*) enantiomer of **2**, which in turn undergoes dimerisation to (+)-oxanthromicin (**1**). Acid-mediated dehydration of **2** could deliver an achiral carbocation intermediate that is reversibly quenched with either H_2O or MeOH to yield (±)–*hemi*-oxanthromicin A (**2**) or B (**3**) respectively. Significantly, the carbocation intermediate could also transform, via a mechanism foreshadowed in a 1979 study directed at the acid-mediated dimerisation of 10-methyleneanthrone,[6] to yield a (±)-*spiro*-carbocation. The (±)-*spiro*-carbocation could in turn undergo reversible quenching with either MeOH or H_2O to deliver the diastereomeric (±)-*spiro*-oxanthromicin B1 (**5**) and B2 (**6**), or the diastereomeric (±)-*spiro*-oxanthromicin C1 (**7**) and C2 (**8**), respectively. Finally, the acid-labile doubly benzylic 10-OH moiety in **7** and **8** can undergo irreversible dehydration to yield (±)-*spiro*-oxanthromicin A (**4**) as a stable quinone methide. In addition to rationalising the biosynthetic/chemical relationships between

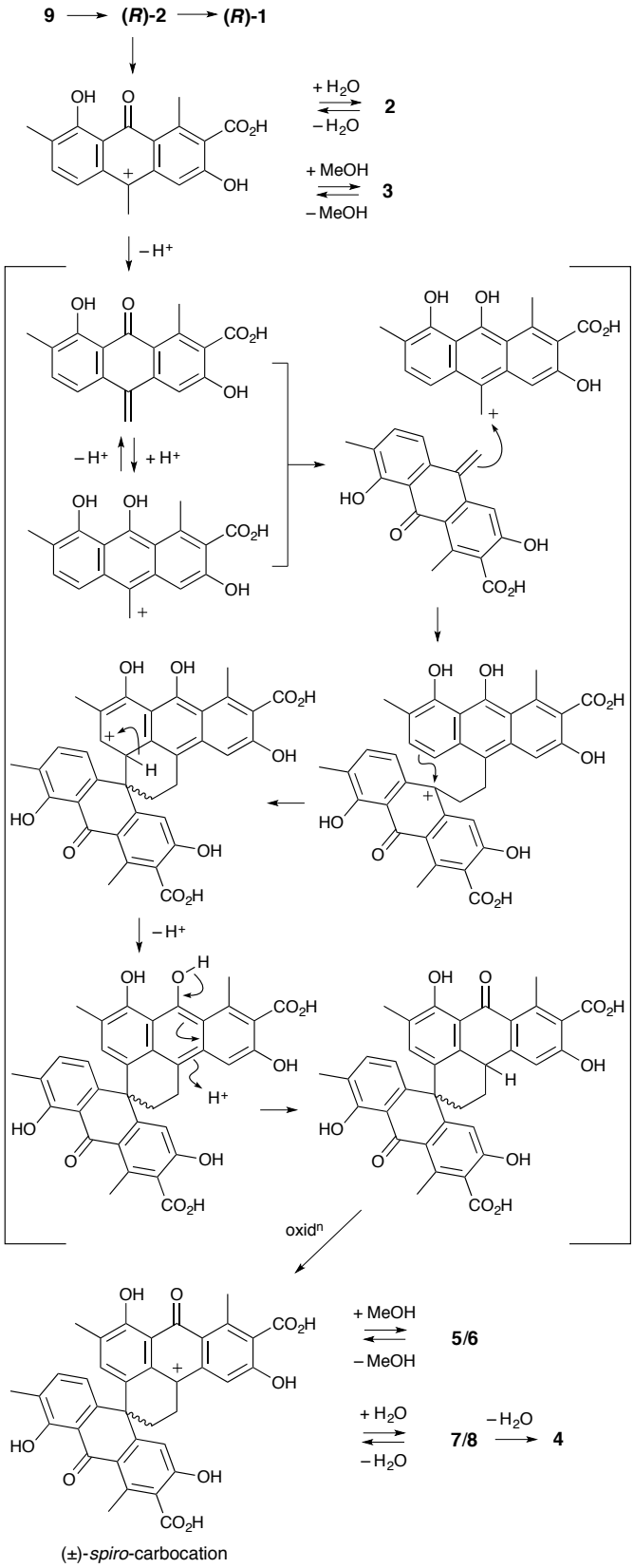

Fig. 4 Biosynthetic/chemical pathway linking **1**–**9**

1–**9**, this biosynthetic/chemical pathway demonstrates for the first time that a rare *spiro* dimerisation mechanism, first proposed in 1979,[6] has a footprint in the natural world.

To support the structural assignments outlined above, and to provide material for a structure activity relationship (SAR) study, we embarked on the syntheses summarised in Scheme 1. Commercially available 2,4-dichloro-1,4-benzoquinone was treated with the Danishefsky diene derived from tiglic aldehyde[7] to form a Diels-Alder adduct, which on Jones oxidation yielded 2-chloro-8-hydroxy-7-methylnaphthaquinone[8] (60%). A subsequent Diels-Alder reaction with the Danishefsky diene derived from ethyl diacetoacetate[9] yielded oxanthroquinone ethyl ester (**11**) (58%) (ESI Figs. S6a–S6b), which on hydrolysis returned oxanthroquinone (**9**) (88%). Treatment of synthetic **9** with MeMgBr resulted in regioselective addition to C-10 in preference to C-9, which is chelated to the adjacent 8-hydroxy, to yield (±)-*hemi*-oxanthromicin A (**2**) (45%). NMR data showed that synthetic samples **9** and **2** are identical in all respects to the natural products. As the stability studies discussed above had established a sequence of chemical transformations from **2** to **3**–**8**, the total synthesis of **9** and **2** represents a formal synthesis of **3**–**8.** To further explore SAR, we exploited the chelation of 8-OH to selectively monomethylate **11** with MeI (Scheme 1) to yield 3-*O*-methyl oxanthroquinone ethyl ester (**14**) (72%) (ESI Figs. S7a–S7b).

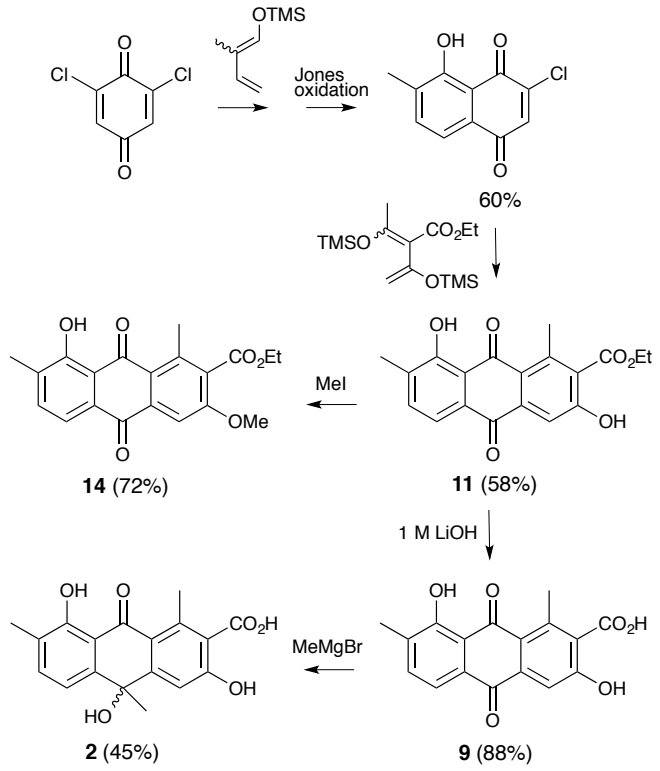

Scheme 1. Synthesis of **2**, **9**, **11**, and **14**.

On reviewing the polyketide natural products literature, we noted **1**–**9** possess unique 1-Me/7-Me and 2-CO_2H substitutions. To explore the possible SAR significance of the 7-Me and 2-CO_2H moieties, we completed the syntheses outlined in Scheme 2, transforming 3-bromojuglone to 7-desmethyloxanthroquinone ethyl ester (**12**) (68%) (ESI Figs. S8a–S8b) and 7-desmethyloxanthroquinone (**13**) (90%) (ESI Figs. S9a–S9b).

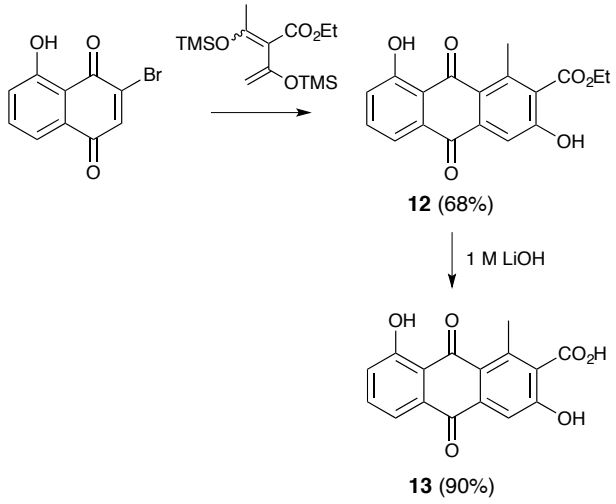

Scheme 2. Synthesis of **12** and **13**

We next set out to use quantitative confocal imaging to measure the ability of **1**–**2**, **4**, **9** and **11**–**14** to mislocalise oncogenic mutant K-Ras (mGFP-K-RasG12V) from the PM of intact Madin-Darby canine kidney (MDCK) cells following a previously published protocol.[4] The results (Table 1) revealed that the natural product (+)-oxanthromicin (**1**), the dimeric transformation product (±)-*spiro*-oxanthromicin A (**4**) and the synthetic ethyl ester analogues **12**, **11** and **14** (in increasing order of potency) were effective at mislocalising K-Ras from the PM. An SAR analysis of these data suggests that the monomers **11** and **12**–**14** are more active than the dimers **1** and **4**, and that esterification of the 2-CO_2H moiety improves K-Ras mislocalisation. Activity is further enhanced by the presence of a 7-Me, and substitution (methylation) of the 3-OH.

Table 1. Summary of K-Ras mislocalisation studies

Compound	E_{max} ± SEM	IC_{50} (μM) ± SEM
1	0.76±0.02	62.5±8.0
2	0.47±0.03	[a]
4	0.75±0.03	26.7±7.2
9	0.44±0.05	[a]
11	0.76±0.04	4.6±0.8
12	0.73±0.02	18.6±2.9
13	0.43±0.02	[a]
14	0.73±0.02	1.2±0.3
10	0.67±0.03	0.00051±0.0002

[a] Compounds with an $E_{max} < 0.50$ were deemed to be inactive. Negative control DMSO $E_{max} = 0.37$.

To further our investigations into oxanthromicin/oxanthroquinone chemistry and biology, we analysed our in-house database of the HPLC-DAD secondary metabolite profiles of ~50,000 microbial extracts, to detect additional *Streptomyces* capable of producing examples of this

structure class. This study revealed two *Streptomyces* that were subsequently re-cultivated and subjected to detailed chemical analysis. *Streptomyces* sp. MST-RA9773 isolated from a soil sample collected near Barellan, New South Wales (NSW), and *Streptomyces* sp. MST-104069 isolated from a soil sample collected near Broken Hill, NSW, produced **1** and related *hemi*- and *spiro*-oxanthromicins, only the former produced **10**. This analysis established that oxanthromicins/oxanthroquinone are exceptionally rare with an incidence (in our library) of ~1:17,000, in contrast to staurosporine with an incidence of ~1:100. The repeated co-production of oxanthromicins/oxanthroquinone and staurosporine is noteworthy, and raised the possibility that these structurally diverse microbial metabolites may exhibit synergistic biological properties. To probe this hypothesis, we quantified the K-Ras mislocalising properties of **10** when exposed to sub-IC_{50} doses of **1**–**2**, **4**, **9** or **12**–**13** (4 μM), **11** (1.45 μM) and **14** (0.60 μM), revealing significant levels of synergism by **1** (130%), **4** (750%), **11** (410%) and **14** (470%).

Conclusions

In conclusion, this report describes a successful high-throughput, high-content microbial biodiscovery approach to detect and identify novel small molecule inducers of K-Ras PM mislocalisation. Our chemical investigations of *Streptomyces* sp. MST-134270 yielded a suite of new polyketides **1**–**9**, interconnected by an array of biosynthetic and chemical transformations, inclusive of the first natural occurrence of a rare *spiro* dimerisation reaction. Structure elucidations were supported by detailed spectroscopic analysis, chemical interconversion and total synthesis. SAR studies established the synthetic anthraquinone **14** as a potent lead candidate, capable of mislocalising oncogenic mutant K-Ras (mGFP-K-RasG12V) from the PM of intact MDCK cells. We established the natural occurrence of oxanthromicins/oxanthroquinone (in our library) as being exceptionally low, and correlated with the co-production of staurosporine (**10**). Co-treatment of **10** with sub-EC_{50} doses of selected oxanthoquinones resulted in a significant synergism of K-Ras PM mislocalisation. Collectively, these studies demonstrate that a rare class of *Streptomyces* polyketides, and analogues inspired by these compounds, can induce significant K-Ras PM mislocalisation (IC_{50} 1.2 μM), and can synergise the K-Ras PM mislocalisation properties of staurosporine (IC_{50} 60 pM). A detailed account of the biological properties and mechanism of action of these polyketides will be reported elsewhere.

Experimental section

Microbial Cultivation and Extraction

A *Streptomyces* sp. (MST-134270) cultivation was incubated for 10 days at 28 °C in 40 Erlenmeyer flasks (250 mL each) containing sterilised cracked wheat (50 g) hydrated in water (30 mL), and inoculated with 5 mL of a ISP2 media seed fermentation. The resulting ferment (3.14 kg) was extracted with acetone (6 L), filtered and concentrated *in vacuo* to an aqueous concentrate (800 mL). The aqueous concentrate was extracted with EtOAc (1.5 L) and concentrated *in vacuo* to yield a crude EtOAc extract (7.2 g), which was subsequently partitioned between hexane and MeOH to give hexane-soluble (2.4 g) and MeOH-soluble (4.8 g) extracts (ESI Scheme S1).

Fractionation and characterisation of compounds

A portion of MeOH-soluble extract (206 mg) was fractionated using a C_{18}-max SPE cartridge (5 g) eluting with a stepwise gradient from 90% H_2O/MeOH to 100% MeOH with isocratic 0.01% TFA modifier to give Fractions A–G. SPE Fraction E (62 mg), eluting at 30% H_2O/MeOH, was further fractionated by semi-preparative HPLC (Agilent Zorbax XDB-C_8, 5 μm, 9.4 × 250 mm column, 10 min gradient elution at 3.5 mL/min from 70–20% H_2O/MeCN, then 100% MeCN for 5 min, with isocratic 0.01% TFA modifier) to afford staurosporine (**10**) (t_R 4.8 min, 16.0 mg), (±)-*hemi*-oxanthromicin A (**2**) (t_R 8.1 min, 17.1 mg) and (±)-*hemi*-oxanthromicin B (**3**) (t_R 10.1 min, 2.9 mg). SPE Fraction F (40 mg), eluting at 15% H_2O/MeOH, was further fractionated by semi-preparative HPLC (Agilent Zorbax XDB-C_8, 5 μm, 9.4 × 250 mm column, 12 min gradient elution at 3.5 mL/min, from 50–20% H_2O/MeCN with isocratic 0.01% TFA modifier) to afford staurosporine (**10**) (t_R 2.8 min, 7.5 mg), (±)-*hemi*-oxanthromicin A (**2**) (t_R 5.2 min, 8.0 mg), oxanthroquinone (**9**) (t_R 6.5 min, 2.0 mg), (±)-*hemi*-oxanthromicin B (**3**) (t_R 7.5 min, 5.1 mg), (±)-*spiro*-oxanthromicin B1 (**5**)* (t_R 9.0 min, 2.0 mg), (±)-*spiro*-oxanthromicin A (**4**) (t_R 9.8 min, 1.8 mg), (±)-*spiro*-oxanthromicin B2 (**6**)* (t_R 10.6 min, 1.5 mg). (*Note: **5** and **6** transformed to the more stable **4** during the removal of HPLC solvents). SPE Fraction G (55 mg), eluting with MeOH, was further fractionated by semi-preparative HPLC (Agilent Zorbax XDB-C_8, 5 μm, 9.4 × 250 mm column, 12 min gradient elution at 3.5 mL/min, from 60% H_2O/MeCN to 100% MeCN with isocratic 0.01% TFA modifier) to afford staurosporine (**10**) (t_R 3.5 min, 5.5 mg), (±)-*hemi*-oxanthromicin A (**2**) (t_R 6.2 min, 0.7 mg), (±)-*hemi*-oxanthromicin B (**3**) (t_R 8.2 min, 1.8 mg), (±)-*spiro*-oxanthromicin A (**4**) (t_R 9.7 min, 2.3 mg) and (+)-oxanthromicin (**1**) (t_R 11.4 min, 13.7 mg) (ESI Scheme S1). Based on the above, the estimated % yield from the crude culture extract is **1** (0.99%), **2** (1.9%), **3** (0.71%), **4** (0.30%), **5** (0.14%), **6** (0.11%), **9** (0.15%) and **10** (2.1%) (Note: these yields do not take into account the transformation of **2** to **3** and **4**; **3** to **2**; **5** and **6** to **4** after HPLC purification). (ESI Figs. S13–S14).

(+)-oxanthromicin (1): Yellow amorphous solid; $[\alpha]_D^{22}$ +157 (*c*=0.26, EtOH); UV (MeOH) λ_{max} (log ε) 259 (4.34), 321 (4.31), 355 (4.22) nm; NMR (DMSO-d_6) see ESI Table S1 and Figs. S1a–S1b; HRESI(–)MS *m/z* 653.1662 $[M–H]^-$ (calcd for $C_{36}H_{29}O_{12}^-$, 653.1664)

(±)-*hemi*-oxanthromicin A (2): Yellow amorphous solid; $[\alpha]_D^{22}$ 0 (*c*=0.10, EtOH); UV (MeOH) λ_{max} (log ε) 259 (4.05), 325 (4.02), 341 (3.99), 356 (3.96) nm; NMR (DMSO-d_6) ESI Table S2 and Figs. S2a–S2b; HRESI(–)MS *m/z* 327.0882 $[M–H]^-$ (calcd for $C_{18}H_{15}O_6^-$, 327.0874).

(±)-*hemi*-oxanthromicin B (3): Yellow amorphous solid; $[\alpha]_D^{22}$ 0 (*c*=0.13, EtOH); UV (MeOH) λ_{max} (log ε) 258 (4.12), 323 (4.10), 344 (4.04), 355 (4.03) nm; NMR (DMSO-d_6) ESI Table S3 and Figs. S3a–S3b; HRESI(–)MS *m/z* 341.1029 $[M–H]^-$ (calcd for $C_{19}H_{17}O_6^-$, 341.1031).

(±)-*spiro*-oxanthromicin A (4): Yellow amorphous solid; $[\alpha]_D^{22}$ 0 (*c*=0.13, EtOH); UV (MeOH) λ_{max} (log ε) 239 (4.55), 258 (4.48), 303 (4.38), 356 (4.18) nm; NMR (DMSO-d_6) ESI Table S4 and Figs. S4a–S4b; HRESI(–)MS *m/z* 617.1450 $[M–H]^-$ (calcd for $C_{36}H_{25}O_{10}^-$, 617.1453).

(±)-*spiro*-oxanthromicin B1 (5): UV (MeCN/H_2O) λ_{max} 235, 275, 320, 360 nm; HRESI(–)MS *m/z* 649.1739 $[M–H]^-$ (calcd for $C_{37}H_{29}O_{11}^-$, 649.1715).

(±)-*spiro*-oxanthromicin B2 (6): UV (MeCN/H_2O) λ_{max} 235, 275, 320, 360 nm; HRESI(–)MS *m/z* 649.1735 $[M–H]^-$ (calcd for $C_{37}H_{29}O_{11}^-$, 649.1715).

(±)-*spiro*-oxanthromicin C1 (7): UV (MeCN/H_2O) λ_{max} 235, 275, 320, 360 nm; HRESI(–)MS *m/z* 635.1565 $[M–H]^-$ (calcd for $C_{36}H_{27}O_{11}^-$, 635.1559).

(±)-*spiro*-oxanthromicin C2 (8): UV (MeCN/H_2O) λ_{max} 235, 275, 320, 360 nm; HRESI(–)MS *m/z* 635.1559 $[M–H]^-$ (calcd for $C_{36}H_{27}O_{11}^-$, 635.1559).

oxanthroquinone (9): Orange amorphous solid; UV (MeOH) λ_{max} (log ε) 221 (4.19), 284 (4.14), 412 (3.53) nm; NMR (DMSO-d_6) ESI Table S5 and Figs. S5a–S5b; HRESI(–)MS *m/z* 311.0568 $[M–H]^-$ (calcd for $C_{17}H_{11}O_6^-$, 311.0561).

Chemical stability studies of 1–4

Aliquots of **1**–**4** (0.1 mg) were dissolved in either 0.1% TFA in MeCN (0.5 mL) or 0.1% TFA in MeOH (0.5 mL) and heated at 40 °C for 24 h, after which the solutions were analysed by HPLC-DAD-MS (Agilent Zorbax SB-C_8, 5 μm, 4.6 × 150 mm column, 15 min gradient elution at 1 mL/min from 90% H_2O/MeCN to 100% MeCN with isocratic 0.05% formic acid modifier). Samples of **1**–**4** (0.1 mg) dissolved in MeOH (1.0 mL) were used as authentic standards, and analysed by the same HPLC method. Analytical results, as illustrated in the ESI Figs. S12–S14, demonstrate that whereas **1** and **4** were stable under these conditions, **2** and **3** equilibrate, and transform through **5** and **6**, to **7** and **8**, and finally to **4**.

Synthetic studies

2-chloro-8-hydroxy-7-methylnaphthaquinone: A solution of 2,4-dichloro-1,4-benzoquinone (354 mg, 2.00 mmol) and the Danishefsky diene derived from tiglic aldehyde[7] (340 mg, 2.18 mmol) in toluene (5 mL) was stirred at r.t. for 1 h. After concentrating *in vacuo*, the residue was dissolved in acetone and stirred at r.t. for 16 h in the presence of Jones reagent (2.5 M CrO_3 in 3.6 M H_2SO_4) (5.0 mL, 12.5 mmol). After quenching excess reagent by addition of 2-propanol (10 mL) the reaction mixture was filtered, extracted with Et_2O (20 mL), and the organic phase washed with H_2O (10 mL) and brine (10 mL). The residue recovered from concentrating *in vacuo* was recrystallised from EtOAc to afford 2-chloro-8-hydroxy-7-methylnaphthaquinone[8] (266 mg, 60% for 2 steps). ^{1}H NMR (600 MHz, $CDCl_3$): δ_H = 12.06 (s, 1H), 7.56 (d, *J* = 7.7 Hz, 1H), 7.53 (d, *J* = 7.7 Hz, 1H), 7.17 (s, 1H), 2.37 (s, 3H).

oxanthroquinone ethyl ester (11): A solution of 2-chloro-8-hydroxy-7-methylnaphthaquinone (80 mg, 0.36 mmol) and the Danishefsky diene derived from ethyl diacetoacetate[9] (230 mg, 0.72 mmol) in toluene (5 mL) was refluxed for 3 days. After concentrating *in vacuo* the residue was extracted with CH_2Cl_2 (5 mL) and stirred in the presence of silica gel (240 mg) at r.t. for 5 min. The reaction mixture was then concentrated *in vacuo* and the residue purified by silica gel chromatography (isocratic elution 1:10 EtOAc:light petroleum) to afford oxanthroquinone ethyl ester (**11**) (R_f 0.4; 71 mg, 58%). UV (MeOH) λ_{max} (log ε) 221 (4.50), 273 (4.58), 414 (3.93) nm; ^{1}H NMR (600 MHz, $CDCl_3$): δ_H =13.28 (s, 1H), 10.49 (s, 1H), 7.78 (s, 1H), 7.69 (d, *J* = 7.6 Hz, 1H), 7.49 (d, *J* = 7.6 Hz, 1H), 4.53 (q, *J* = 7.2 Hz, 1H), 2.99 (s, 3H), 2.38 (s, 3H), 1.48 (t, *J* = 7.2 Hz, 3H); ^{13}C NMR (150 MHz, DMSO-d_6): δ_C = 189.6, 181.6, 166.8, 160.0, 158.9, 141.0, 136.8, 136.5, 134.6, 130.2, 129.8, 122.4, 118.1, 115.7, 112.0, 61.5, 19.9, 15.9, 14.1 (ESI Figs. S6a–S6b); HRESI(–)MS *m/z* 339.0873 $[M–H]^-$ (calcd for $C_{19}H_{15}O_6^-$, 339.0874).

oxanthroquinone (9): A solution of **11** (70 mg, 0.21 mmol) in aq. LiOH (1 M; 2 mL) was stirred at 100 °C overnight. The dark red solution was then acidified by addition of aq. HCl (1 M; 2.1 mL) and extracted with Et_2O (3 × 5 mL). The organic phase was dried over anhydrous $MgSO_4$, concentrated *in vacuo* and purified using a C_{18} SPE cartridge (stepwise gradient of 90% H_2O/MeCN to 100% MeCN) to afford synthetic oxanthroquinone (**9**; 56 mg, 88%) identical in all respects to natural **9**.

(±)-*hemi*-oxanthromicin A (2): A solution of **9** (20 mg, 0.064 mmol) in anhydrous THF (1 mL) was cooled to 0 °C and MeMgBr (3 M in Et_2O; 430 μL, 1.3 mmol) was added. The mixture was allowed to reach r.t. and then stirred overnight. After quenching with sat. aqueous NH_4Cl, the reaction mixture was acidified to pH 4 with 0.1 M HCl and extracted with Et_2O (3 × 3 mL), after which the organic phase was dried over anhydrous $MgSO_4$, concentrated *in vacuo*, and purified by semi-preparative HPLC [Agilent Zorbax Rx-C_8, 5 μm, 9.4 × 250 mm column, 15 min gradient elution at 3.5 mL/min from 90% H_2O/MeCN to 100% MeCN with isocratic 0.01% TFA modifier] to afford synthetic (±)-*hemi*-oxanthromicin A (**2**; t_R 10.9 min, 8.3 mg, 45%), identical in all respects to natural **2**, and recovered oxanthroquinone (**9**; t_R 11.9 min, 9 mg, 43%).

3-O-methyl oxanthroquinone ethyl ester (14): A solution of **11** (6.0 mg, 0.018 mmol) and K_2CO_3 (5.0 mg, 0.035 mmol) in acetone (1 mL) was treated with MeI (6.0 mg, 0.042 mmol) and stirred overnight at r.t. The filtered reaction mixture was acidified to pH 4 with 0.1 M HCl and extracted with Et_2O (3 × 3 mL), and the organic phase dried over anhydrous $MgSO_4$, concentrated *in vacuo*, and purified by preparative HPLC [Phenomenex Luna C_{18} (2), 10 μm, 21.2 × 250 mm column, 15 min gradient elution at 20 mL/min from 90% H_2O/MeCN to 100% MeCN with isocratic 0.01% TFA modifier] to afford 3-*O*-methyl-oxanthroquinone ethyl ester (**14**; t_R 16.9 min, 4.5 mg, 72%). UV (MeOH) λ_{max} (log ε) 222 (4.70), 270 (4.72), 298

(4.28), 415 (3.94) nm; ^{1}H NMR (600 MHz, $CDCl_3$): δ_H = 13.25 (s, 1H), 7.75 (s, 1H), 7.69 (d, *J* = 7.7 Hz, 1H), 7.48 (d, *J* = 7.7 Hz, 1H), 4.46 (q, *J* = 7.2 Hz, 1H), 4.01 (s, 3H), 2.76 (s, 3H), 2.37 (s, 3H), 1.41 (t, *J* = 7.2 Hz, 3H); ^{13}C NMR (150 MHz, $CDCl_3$): δ_C = 190.3, 182.5, 167.3, 161.1, 160.0, 141.4, 137.8, 136.5, 135.8, 131.5, 130.6, 125.0, 118.8, 116.2, 107.6, 62.1, 56.6, 20.2, 16.5, 14.3 (ESI Figs. S7a–S7b); HRESI(+)MS *m/z* 377.0997 $[M+Na]^+$ (calcd for $C_{20}H_{18}O_6Na^+$, 377.0996).

7-desmethyloxanthroquinone ethyl ester (12): A solution of 3-bromojuglone[10] (100 mg, 0.40 mmol) and the Danishefsky diene derived from ethyl diacetoacetate[9] (250 mg, 0.79 mmol) in toluene (5 mL) was refluxed for 3 days. After concentrating *in vacuo* the residue was dissolved in CH_2Cl_2 (5 mL), stirred with silica gel (250 mg) at rt for 5 min, concentrated *in vacuo* and purified by silica gel chromatography (isocratic elution 1:10 EtOAc:light petroleum) to afford 7-desmethyl-oxanthroquinone ethyl ester (**12**; R_f 0.4; 88 mg, 68%).[11] UV (MeOH) λ_{max} (log ε) 220 (4.20), 272 (4.26), 409 (3.47) nm; ^{1}H NMR (600 MHz, $CDCl_3$): δ_H = 12.93 (s, 1H), 10.53 (s, 1H), 7.79 (s, 1H), 7.78 (dd, *J* = 7.5, 1.0 Hz, 1H), 7.62 (dd, *J* = 8.3, 7.5 Hz, 1H), 7.31 (dd, *J* = 8.3, 1.0 Hz, 1H), 4.54 (q, *J* = 7.2 Hz, 1H), 2.99 (s, 3H), 1.48 (t, *J* = 7.2 Hz, 3H); ^{13}C NMR (150 MHz, $CDCl_3$): δ_C = 189.6, 182.2, 170.1, 163.6, 162.5, 148.0, 138.7, 135.8, 132.7, 125.0, 124.5, 121.2, 118.9, 117.5, 115.1, 62.9, 21.9, 14.1 (ESI Figs. S8a–S8b); HRESI(–)MS *m/z* 325.0719 $[M–H]^-$ (calcd for $C_{18}H_{13}O_6^-$, 325.0718).

7-desmethyloxanthroquinone (13): A solution of **12** (48 mg, 0.15 mmol) in aq. LiOH (1 M; 1 mL) was stirred at 100 °C overnight. The dark red solution was acidified by aq. HCl (1 M; 1.05 mL) and extracted with Et_2O (2 × 5 mL), after which the organic phase was dried over anhydrous $MgSO_4$, concentrated *in vacuo*, and purified using a C_{18} SPE cartridge (stepwise gradient of 90% H_2O/MeCN to 100% MeCN) to afford 7-desmethyl-oxanthroquinone (**13**; 39 mg, 90%).[12] UV (MeOH) λ_{max} (log ε) 217 (4.68), 280 (4.72), 411 (4.08) nm; ^{1}H NMR (600 MHz, DMSO-d_6): δ_H = 12.89 (s, 1H), 7.76 (dd, *J* = 8.3, 7.5 Hz, 1H), 7.66 (dd, *J* = 7.5, 1.1 Hz, 1H), 7.60 (s, 1H), 7.36 (dd, *J* = 8.3, 1.1 Hz, 1H), 2.71 (s, 3H); ^{13}C NMR (150 MHz, DMSO-d_6): δ_C = 189.4, 182.1, 168.3, 161.5, 159.2, 140.9, 136.4, 136.2, 132.5, 131.2, 124.5, 122.5, 118.4, 116.9, 112.2, 20.0 (ESI Figs. S9a–S9b); HRESI(–)MS *m/z* 297.0405 $[M–H]^-$ (calcd for $C_{16}H_9O_6^-$, 297.0405).

K-Ras bioassay

Madin-Darby canine kidney (MDCK) cells stably co-expressing monomeric green fluorescent protein (mGFP) coupled to the N-terminus of oncogenic K-Ras (K-RasG12V) and mCherry-CAAX, a red fluorescent fusion protein that decorates endomembranes,[4] were plated at 150,000 cells/well on 12-well plates. After 24 h, cells were treated with compounds and incubated for another 48 h. Each compound was tested in 3 independent experiments. At the end of incubation time, cells were fixed with 4% paraformaldehyde and imaged in a Nikon A1R confocal microscope. Ras mislocalisations from the plasma membranes were calculated using Manders coefficients, by measuring the fraction of mCherry-CAAX co-localizing with mGFP-K-RasG12V.[4] IC_{50} values and two-tailed t-tests were calculated using Prism software (Ver. 5.0c, GraphPad). E_{max} quantifies the maximum extent of mislocalisation of K-Ras from the plasma membrane to endomembrane.

Acknowledgements

We acknowledge the assistance of A. Crombie (MST) in the fermentation and genetic sequencing of isolates, and A. Lacey (MST) in the extraction and purification of metabolites. This research was funded in part by the Australian Research Council (ARC DP120100183 and LP120100088), The University of Queensland, the Institute for Molecular Bioscience, and the Cancer Prevention and Research Institute of Texas (RP100483).

Notes and references

[a] Institute for Molecular Bioscience, The University of Queensland, St. Lucia, QLD, 4072, Australia.
[b] Integrative Biology and Pharmacology, The University of Texas Medical School, Houston, Texas 77030, USA.
[c] Microbial Screening Technologies Pty. Ltd. Building C, 28-54 Percival Rd. Smithfield, NSW 2164, Australia.
‡ These two authors contributed equally to this paper.
† Present address: Department of Chemistry and Biomolecular Sciences, Macquarie University, NSW 2109, Australia

* Corresponding author. Fax: +61-7-3346-2090; Tel: +61-7-3346-2979; E-mail: r.capon@uq.edu.au.

Electronic Supplementary Information (ESI) available: General experimental details, full details of microbial collection and taxonomy, tabulated 2D NMR data and NMR spectra and LCMS stability studies. See DOI: 10.1039/b000000x/

1 J. F. Hancock, *Nat. Rev. Mol. Cell Biol.* 2003, **4**, 373.
2 B. O. Bodemann and M. A. White, *Curr. Biol.* 2013, **23**, R17.
3 A. T. Baines, D. Xu and C. J. Der, *Future Med. Chem.* 2011, **3**, 1787.
4 K.-j. Cho, J.-H. Park, A. M. Piggott, A. A. Salim, A. A. Gorfe, R. G. Parton, R. J. Capon, E. Lacey and J. F. Hancock, *J. Biol. Chem.* 2012, **287**, 43573.
5 (a) M. Patel, A. C. Horan, V. P. Gullo, D. Loebenberg, J. A. Marquez, G. H. Miller and J. A. Waitz, *J. Antibiot.* 1984, **37**, 413; (b) J. J. K. Wright, Y. Merill, M. S. Puar and A. T. mcPhail, *J. Chem. Soc., Chem. Commun.* 1984, 473.
6 H. D. Becker and D. Sanchez, *J. Org. Chem.* 1979, **44**, 1787.
7 M. T. Gieseler and M. Kalesse, *Org. Lett.* 2011, **13**, 2430.
8 L. Boisvert and P. Brassard, *J. Org. Chem.* 1988, **53**, 4052.
9 B. Caron and P. Brassard, *Tetrahedron* 1993, **49**, 771.
10 L. F. Tietze, R. R. Singidi and K. M. Gericke, *Chem. Eur. J.* 2007, **13**, 9939.
11 S. J. Bingham and J. H. P. Tyman, *J. Chem. Soc. Perkin Trans. 1* 1997, 3637.
12 T. S. Lee, A. Das and C. Khosla, *Bioorg. Med. Chem.* 2007, **15**, 5207.